Ann. Geophys., 27, 1313–1320, 2009
www.ann-geophys.net/27/1313/2009/
© Author(s) 2009. This work is distributed under
the Creative Commons Attribution 3.0 License.

Annales Geophysicae

Magnetic-inclination effects in the spectral resonance structure of the ionospheric Alfvén resonator

T. Bösinger[1], **E. N. Ermakova**[2], **C. Haldoupis**[3], **and D. S. Kotik**[2]

[1]University of Oulu, Department of Physical Sciences, Oulu, Finland
[2]Radio Physical Institute, Nizhny Novgorod, Russia
[3]University of Crete, Physics Department, Heraklion, Crete, Greece

Received: 19 September 2008 – Revised: 6 January 2009 – Accepted: 14 January 2009 – Published: 13 March 2009

Abstract. Based on recent developments in the formalism governing the spectral resonance structures (SRS) of the Ionospheric Alfvén resonator (IAR) as observed on the Earth's surface, a numerical code was developed to investigate properties of SRS which can in particular be contributed to magnetic inclination effects. Among the theoretical findings are: 1) SRS is discernible in both orthogonal components, 2) the harmonic structure of SRS is not anymore over frequency equidistantly distributed, 3) the frequency scales of SRS differ in the two normal modes. The theoretically predicted properties could be found in the observations of a low latitude and some of them even in the data of a mid latitude station. The verification, however, is not as straight forward because the predicted effects do not only depend on magnetic inclination but also on the wave angle of the lightning induced electromagnetic wave k-vector with the normal to the magnetic meridian passing through the observation site. So far the formalism is simplified as it deals with a single source situation alone whereas the actual observation is a composite of excitations caused by an average of about 60 flashes of lightning operating all the time, world-wide.

Keywords. Ionosphere (Ionosphere-atmosphere interactions) – Radio science (Electromagnetic noise and interference) – Space plasma physics (Kinetic and MHD theory)

1 Introduction

Since the pioneering works by Polyakov (1976), Polyakov and Rapoport (1981) and Belyaev et al. (1987) the discovery of the ionospheric Alfvén resonator (IAR) led to a manifold of investigations including direct and indirect manifestations of IAR and its role in the atmospheric, ionospheric and magnetospheric context. The basic physics behind the IAR phenomenon, which is well known, is summarized by (Demekhov et al., 2000) and thus will not be repeated here. Among the IAR issues under research are: various excitation mechanisms (e.g. Sukhorukov and Stubbe, 1997; Surkov et al., 2004, 2006; Shalimov and Bösinger, 2008), latitudinal and longitudinal degree of localisation (Pokhotelov et al., 2003; Semenova and Yahnin, 2008), appearance in extreme regions, such as low latitude and polar cap (e.g. Bösinger et al., 2002; Semenova and Yahnin, 2008), usage in ionospheric diagnostics (e.g. Hebden et al., 2005; Odzimek et al., 2006), IAR's role in atmospheric, ionospheric, magnetospheric coupling (e.g. Lysak, 1993; Demekhov et al., 2000; Bösinger and Shalimov, 2008), non-linear effects (e.g. Trakhtengerts and Feldstein, 1991; Lysak, 1993; Pokhotelov et al., 2003), and artificial excitation (e.g. Bösinger et al., 2000; Scoffield et al., 2006). The present paper is the first dealing with magnetic inclination effects which are expected to be detectable at low latitudes. To our knowledge this issue has not so far been addressed in the literature besides a national report, today available in a version translated into English (Ermakova et al., 2008).

In the following, first some details of the ground-based observations carried out on the island of Crete/Greece between 1999 and 2006 and at a mid latitude station in Russia are presented. Next the formalism and numerical approach of the theoretical investigation are described, followed by a summary of the main magnetic inclination signatures in the spectral resonance structure (SRS) of IAR as derived by a proposed theory. Next, some examples of the observed SRS signatures, which appear to be in tune with our theoretical predictions, are presented. Finally, the paper closes with a brief discussion and a summary of the main points.

Correspondence to: T. Bösinger
(tilmann.bosinger@oulu.fi)

Published by Copernicus Publications on behalf of the European Geosciences Union.

2 Instruments and data processing

From May 1999 till February 2006 the University of Oulu in cooperation with the University of Crete operated a pulsation magnetometer at the island of Crete/Greece. This instrument, as well as a similar one in Russia, we used data from, was of a search-coil type. The geographic coordinates of the observation sites were: in Crete (hereafter referred to as CR) 35.15° N and 25.20° E (magnetic dip angle 51.0°), and in Russia (hereafter referred to as NL) 55.59° N and 45.44° E (dip angle 71.5°). Local time of the former is given by LT=UT+1.5 h, whereas for the latter by LT=UT+3.5 h. We will call NL a mid latitude and CR a low latitude station since with its L-value of only 1.36 CR incorporates already low latitude properties. This classification is also in tune with a nomenclature used earlier (Bösinger et al., 2002). Details on the instrument and data production of CR are given by Bösinger et al. (2002), while the corresponding information on NL can be found in the Appendix to the paper by Belyaev et al. (1990). In general SRS can be described as a weak harmonic modulation in the spectral density of magnetic background noise spectra. If not otherwise mentioned, the spectra shown in the present work are derived from the raw data, since raw data are of advantage in SRS analysis. This is, the increase of sensitivity (induction coil) with frequency counteracts with the decay of spectral density in the natural magnetic background noise. Spectral analyses were done by standard FFT algorithms with parameters given later where necessary.

3 Theory and numerical approach

The magnetic inclination is defined as the angle between the Earth's magnetic field and the horizontal direction at a given altitude. In the following the magnetic inclination angle's complement to 90° is used, that is, the angle between the magnetic field and the vertical. For the sake of simplicity this is called "field angle θ" (in contrast to the "wave angle ϕ" defined later). Further IAR is assumed to be excited mainly by world-wide lightning activity (cf. Shalimov and Bösinger, 2008, and references therein). The starting point is, therefore, the classic VLF theory by Wait (1965), of electromagnetic wave propagation in the Earth-ionosphere waveguide. Due to the very low frequencies in the ULF case, the formalism can be considerably simplified by means of using the quasi-static approach of Belyaev et al. (1989). The two orthogonal horizontal wave-field magnetic components emitted from a single vertical electric dipole (lightning flash) represent the two normal modes, the TM-mode (transversal component, perpendicular to the wave $\boldsymbol{k}$-vector; hereafter referred to as B_ϕ) and the TE mode (longitudinal component, parallel to the $\boldsymbol{k}$-vector; hereafter referred to as B_r). It turns out that, as long as the Earth magnetic field is vertical the B_ϕ-component does not depend on ionospheric parameters. It depends only on the source field intensity (the current moment $I \cdot s$ of the lightning path), the height of the wave guide h, and the distance of the observation point from the source r. It reads:

$$B_\varphi = \frac{\mu_0 \cdot I \cdot s}{2\pi \cdot h \cdot r}, \tag{1}$$

where I stands for current strength and s for the length of the lightning discharge path. In contrast, the longitudinal component B_r is much more complicated as it depends on a large set of ionospheric parameters. It reads (for details see Polyakov et al., 2003):

$$B_r = \frac{\frac{\Sigma_H}{\Sigma_W} \cdot B_\varphi}{\left(\frac{\Sigma_P}{\Sigma_W} \cdot Y\right) - i \cdot k_A \cdot h \cdot \left[\left(\frac{\Sigma_P}{\Sigma_W} + Y\right)^2 + \left(\frac{\Sigma_P}{\Sigma_W}\right)^2\right]} \tag{2}$$

As seen, B_r is direct proportional to local B_ϕ since this is the driving force for excitation of IAR, representing the leakage to the ionosphere above the observation point. In the imaginary part at the denominator, k_A is the Alfvén wave vector in the ionosphere. The symbol Σ stands for height integrated conductivities, and its subscript H, P and W referring to Hall-, Pederson- and Wave impedance, respectively, whereas Y denotes the ionospheric admittance. It is the latter parameter which carries the periodicity (harmonic structure) of IAR. The ionospheric properties are incorporated in B_r because of Alfvén wave leakage back to the atmosphere and its effective coupling to the TE mode. The admittance Y is the inverse of the impedance Z. The influence of the ionosphere enters in Eq. (2) by the impedance Z of the upper boundary of the Earth-ionosphere wave guide.

In this, Polyakov et al. (2003), theoretical approach the magnetic field is assumed to be vertical, which certainly represents a simplification. In the general case of $\theta \neq 0$ the elements in the expression of upper boundary impedance Z (a 2×2 matrix) depend also on the field angle θ. The theory for the $\theta \neq 0$ case was recently developed by Sobchakov et al. (2003) and the numerical code based on their theory and applied to this study is due to Ermakova et al. (2007, 2008, and references therein). For the sake of convenience the lengthy expressions of the transversal and longitudinal wave magnetic field components B_ϕ and B_r are reproduced in the Appendix together with the adopted assumptions. Here attention is drawn to the fact that the introduction of θ, inevitably, leads to the dependence of the field components on the wave angle ϕ, which is defined as the angle between the wave vector k (direction to the source) with the normal to the magnetic meridian passing through the observation site. Of course, all the other dependencies on ionospheric parameters (already existing in Eq. 2) still prevail. An immediate consequence of Eqs. (A1) and (A2) is that the spectral resonance structure SRS of the ionospheric Alfvén resonator, may appear now in both the orthogonal components, B_ϕ and B_r.

It is obvious that for a real ion density ionospheric profile, it is difficult to adopt an analytic expression for the

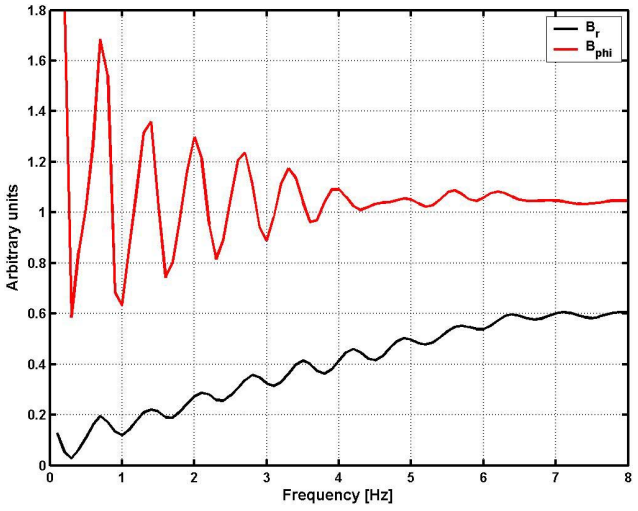

Fig. 1. A theoretical power spectrum in arbitrary units of the transverse B_ϕ, and longitudinal B_r, magnetic field components of an electromagnetic wave (emitted from a single, vertical electric dipole) propagating in the Earth-ionosphere waveguide, as observed at NL (θ=19°), at 18:00 UT on 10 September 2005, assuming a wave angel ϕ=0° and an IRI ionosphere height profile. The harmonic structure seen in both components is a manifestation of a standing wave in the IAR cavity producing a periodicity in the wave guide upper boundary impedance.

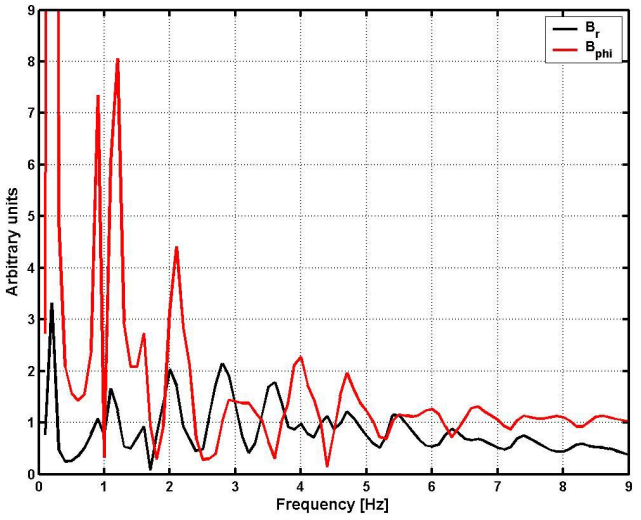

Fig. 2. The same as Fig. 1 but for the station CR and 02:00 UT on 3 January 2000 based on a modified IRI model and the following parameters: θ=39°, ϕ=70°. For more details see text.

impedance Z of the upper boundary of the Earth-ionosphere wave guide. The numerical calculation of Z (cf. Eqs. A4 to A7), starts with a piece-wise computation of the upper boundary impedance at 1000 km height and going downward in steps of 5 km in an iterative process, reaching finally 80 km. In this way, the computed impedance of the upper boundary includes all influences of the upper ionosphere for the wave guide in question.

In the numerical estimates for the present work, three different kinds of ionospheric models were used: The first model used was the IRI (International Reference Ionosphere) model (http://modelweb.gsfc.nasa.gov/ionos/iri.html, e.g., see Reinisch et al., 2007). This model however exhibits at the top side ionosphere a relatively slow decay of ion density with increasing height. In terms of SRS this is unfavourable because a high quality factor Q of the IAR cavity resonance requires a steep decrease of ion density at the topside ionosphere. A second model was a simple Chapman layer topside profile which is characterized by a steep decay, which however is in most cases unrealistic. Finally, a clear SRS was produced in the modelling results, by adopting a more realistic ion density profile resulted by interpolation between the two extremes, the slow decay IRI profile and the steep decay Chapman layer profile. As shown later, a specific type of an ionospheric model is not yet decisive since we are still far from a position where one could strive towards a quantitative determination of SRS.

4 Theoretical assessment

The additional two parameters, the field angle θ and the wave angle ϕ, along with all other ionospheric parameters entering Eq. (2), produce a great variety of different spectra. One basic finding of the theoretical investigation here is that both orthogonal components exhibit SRS signatures. This fact should get discernable even at the mid latitude station NL in spite of its small angle θ as demonstrated by the theoretical estimates shown in Fig. 1. As can be seen, the harmonic structure SRS shows up in both, the B_ϕ and B_r components. It looks like as SRS is more pronounced in the transversal component B_ϕ (which should not exhibit SRS signatures at all for θ=0; cf. Eq. 1). This, however, is misleading because in relative sense the modulation depth in SRS is about equal in both components. In absolute terms B_ϕ is always larger than B_r, since B_ϕ is the driving force of IAR overhead the station.

A survey of SRS as a function of the wave angle ϕ (keeping all other parameters constant) revealed that the modulation depth (difference between maxima and minima) of SRS is smallest and equal in both components for ϕ=45°. Another new feature in SRS is that the resonance lines are not any more necessarily equidistant over the whole frequency range, as in the case when θ=0 (e.g., note the gap between 4 and 6 Hz in the B_ϕ-component of Fig. 1).

As expected the magnetic inclination effects are much more dramatic for the low latitude station CR. Two examples are shown in Figs. 2 and 3, respectively, showing some new spectral features in SRS. These include: an unequal frequency scale (difference Δf in frequency between adjacent resonance frequencies; in the following referred to as FS) in the two orthogonal components, a splitting of the resonance

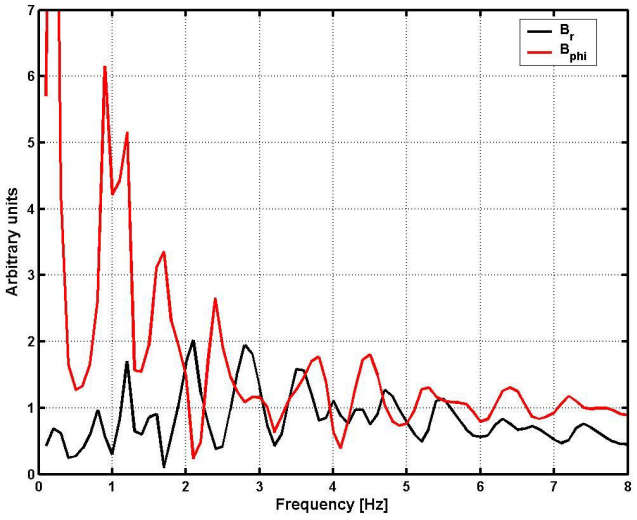

Fig. 3. Same as Fig. 2 but for ϕ=20°. For more details see text.

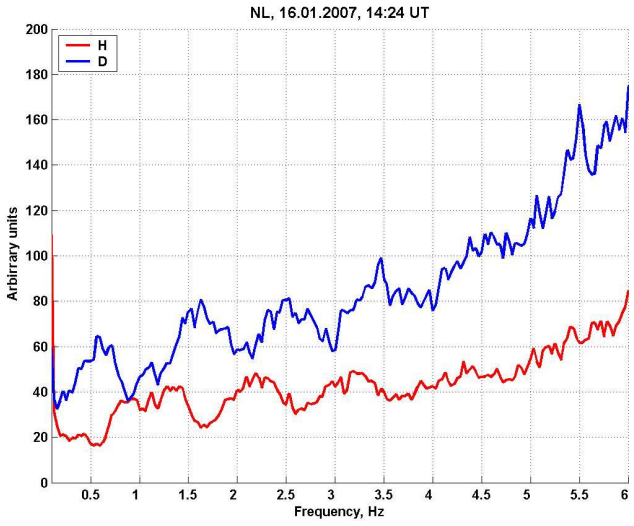

Fig. 4. A power spectrum of the H- and D-component as observed at NL at the given date and time. Averages over successive, non-redundant, 512 point FFTs were used to get an integration over ∼10 min. The general increase of the power spectral density over frequency reflects the increase of sensitivity of the search coil magnetometer (raw data).

lines around 1 Hz, an intermediate small maximum around 1.7 Hz in the B_r-component, and the resonance lines can get very spiky or very broad (B_ϕ-component). By comparing Figs. 2 and 3 one sees that these new effects seem to be mainly governed by the wave angle ϕ. More important, as already noticed in NL (Fig. 1), the resonance lines are not anymore equally spaced over the frequency scale (appearance of gaps).

5 Observations

A large variability in the SRS properties was observed at CR right from the start of operation in 1999 (cf. Bösinger et al., 2002). In general, all the specific features predicted by the present theoretical model were also recognized to be present in the CR observations, although a detailed comparison between theory and experiment is at present not possible. This is because the theory so far deals only with a single electromagnetic emission source (lightning flash), whereas there are on average 60 lightning flashes per second occurring worldwide (e.g. Lyons et al., 1995). In principle, each of them is contributing to the excitation of IAR overhead an observation site. This is particularly true at mid/low latitudes, as compared to high latitudes in which, with regards to SRS, it does not matter which direction the electromagnetic wave from a lightning discharge reaches the observation point. In other words there is no wave angle ϕ dependence for a high latitude station (for a discussion of this point see Demekhov et al., 2000).

As seen, by comparing Figs. 1 to 3, it is the angle ϕ which determines to a high degree the SRS properties at low latitudes, as for instance in CR. Having this in mind one may wonder why it is at all possible to detect in CR – most of the time – relatively stable SRS signatures. This question will be address in the next section. It should be noted that for a fixed orientation of the pulsation magnetometer sensors (H-component pointing to magnetic north, D-component pointing to magnetic east) we cannot generally distinguish between the principal modes (B_ϕ and B_r) since each of our H- and D-component time series is a mixture of the B_ϕ and B_r contributions. In consequence, if FS of B_ϕ and B_r is different (see above) it may result in any kind of interference pattern depending how strongly each of the normal modes contribute to the overall spectrum and how much FS differs between B_ϕ and B_r.

There are more clear cases, however, where one can test further these arguments, e.g., for the case of a quasi single-source situation that dominates the IAR excitation. This can be a thunderstorm centre not far from the observing station capable of producing an effect and still close enough to clearly dominate more distant contributions. In the following, shown are examples of observed SRS which exhibit clearly signatures of a magnetic inclination effect. The first example that is presented in Fig. 4 is for NL and displays the power spectrum of H- and D-components. As seen, the observation exhibits some kind of anti-correlation between the two magnetic field components' harmonic structures (careful inspection of Fig. 1 reveals that this is also true in the higher frequency section of the numerical simulation shown). We found that this anti-correlation can be produced by our model with a suitable chosen set of parameters.

The following two figures (Figs. 5 and 6) display power spectra seen at CR for two consecutive time periods. The spectra of both figures exhibit properties which can be

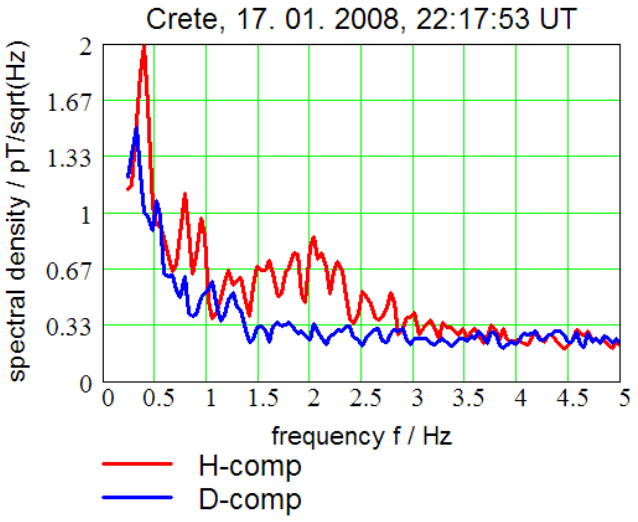

Fig. 5. Magnetic background noise amplitude spectra of CR as observed at the given date and time. The data were corrected for the frequency response of the instrument and calibrated. Eight individual 512 point FFT realisations were averaged resulting in a time resolution of 410 s. The time given refers to the centre of the 410 s time period. The time average is large enough to suppress sufficiently instrumental noise and small enough to guarantee a quasi stationary situation (∼230 registered lightning flashes world-wide in the given time interval according to World Wide Lightning Location Network).

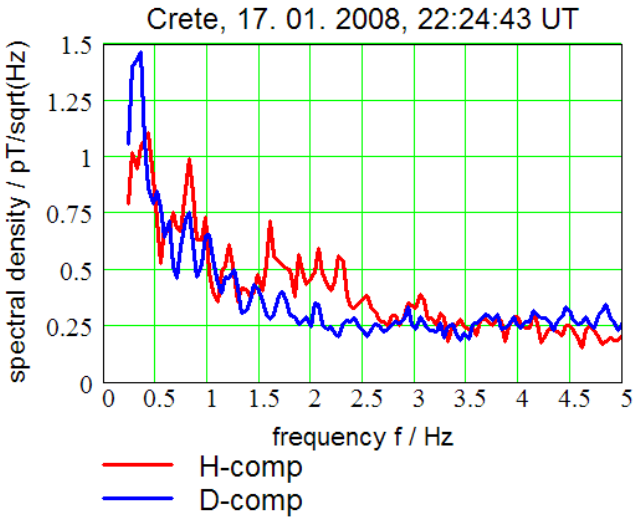

Fig. 6. Same as in Fig. 5 but for the next consecutive 410 s time interval.

interpreted as magnetic inclination effects. In more detail: a) a double resonance peak exists in H between 0.5 and 1.0 Hz (H in Fig. 5) reminding the splitting seen before in Figs. 2 and 3 (pay attention to the saddle point above 1 Hz in the following resonance enhancements and to the subsequent situation shown in Fig. 6), and that the resonance peaks become spiky and broad (especially H in Fig. 6), b) the FS does not anymore match in H and D (especially clear in Fig. 6), c) the resonance peaks are not equally distributed over the frequency range and gaps may occur (e.g. D in Fig. 5), although regular distribution may prevail over a wider frequency range (D in Fig. 6) , d) SRS does appear in both components but each of them lives – so to speak – its own life. The change within 410 s from the situation of Fig. 5 to the one of Fig. 6 demonstrates the large variability of SRS as expected from the theoretical consideration above.

6 Summary, discussion and conclusions

In this work, the essential elements of a recently published theory, dealing with the distant excitation of IAR by a single lightning stroke, were applied to study the effects of the magnetic field inclination on SRS. Starting from this – to our knowledge the most advanced formalism at present – a numerical code was constructed to simulate the ground-based magnetic field observations underneath the excited IAR. A key element in this approach is that the influence of the ionosphere on the electromagnetic wave propagation in the Earth-ionosphere waveguide is fully incorporated in the expression for the impedance of the upper boundary. Using realistic modifications of the IRI model, numerous artificial power spectra of ground-based ULF magnetic field observations at two observing stations, a mid and a low latitude ones, were computed. This allowed us to study in detail the properties of SRS depending on location (latitude), local time, and wave field direction. From this large set of artificial spectra we extracted the most typical and significant SRS properties which could be attributed to a magnetic inclination effect.

For a field angle $\theta \neq 0$, the rotational symmetry with respect to the magnetic field configuration breaks down resulting to a wave angle ϕ dependence with respect to the orientation of the magnetic meridian. The standing Alfvén wave in IAR, responsible for the appearance of SRS, experiences now – so to speak – two slightly different (effective) lengths of magnetic field lines (or different reflection points), depending on whether the horizontal wave vector is within or perpendicular to the magnetic meridian. In other words, with the break-down of rotational symmetry also the wave front's horizontal structure matters. This is a sort of plausible explanation as to why the normal magnetic field components B_ϕ and B_r exhibit different frequency scales (FS). Since the normal modes are coupled, it is now not possible to express the result in simple terms. In general, ground-based observations of the H- and/or D-component of magnetic field variations include a composition of B_ϕ and B_r contributions (different FS), thus phase relationships get important leading to a great variety of SRS.

The comparisons of our numerical results with observations are not as straight forward. For this purpose we should still go one step ahead in our theory by taking into account

the actual distribution of lightning activity world-wide and superpose the contributions from each of the lightning discharges to the overall effect of IAR excitation. The situation is, however, not as hopeless as one may guess form the enormous variability of the SRS properties derived from a single source excitation (see above). For example, the observations made at CR show that sufficiently long integrated SRS spectra are most of the time rather stable. This may be understood realizing that the global distribution of thunderstorm activity changes slowly (neglecting local thunderstorms), on a time scale of roughly an hour. This, as shown by Bösinger et al. (2002), turns out to be in line with the diurnal variations observed in SRS.

In summary, magnetic inclination effects were definitely identified in the present low latitude observations. In addition, it was shown that the magnetic inclination must play a role also at mid latitude. This report is only meant to identify and classify magnetic inclination effects in SRS. This investigation is only half way to the final goal to simulate numerically IAR spectra to such a degree that they can be used, for instance, in ionospheric diagnostics. At present the choice of a specific ionospheric model is not decisive as long as the integral effect of global lightning activity is not incorporated in the numerical simulation. We can say, however, that the determination of FS from the H- and/or D-component's SRS observation does not reflect the "real" FS, since the latter is a composite of the two normal mode, B_ϕ and B_r, frequency scales with an unknown percentage of mixture. It seems that the unequally spaced resonance lines over the frequency make the determination of FS anyway questionable, not to speak about the high variability of SRS from one time instant to the next. Here, a global simulation may help to define a proper integration time to reach trustworthy average values. In some specific cases of SRS patterns, however, a single source situation may exist. This is when, for example, the modulation depth of SRS in H and D is of equal size and the spectral lines between H and D are anti-correlated. Intermediate maxima and spiky resonance structures and obvious gaps are clear signatures of magnetic inclination.

An interesting aspect of our theoretical spectra opens up in the context of fine structure found in SRS observed in CR, and reported earlier (Bösinger et al., 2004). Our artificial SRS showed occasionally also signatures of a fine structure over certain frequency bands. We did not follow up this issue for this report but, in view of the present work, the following question arises: can a specific global distribution of thunderstorm centres produce fine structure in SRS? No doubt, further studies are needed to explain in greater detail low latitude observations of SRS.

Appendix A

Mathematical background

In the case of a finite field angle θ the formulae corresponding to Eqs. (1) and (2) read

$$B_\varphi = \frac{i\cdot\mu_0(I\cdot s)}{2\pi\cdot r\cdot h}\{1+\frac{\delta_1\sin(2\varphi)(\kappa+2\delta_1\sin(2\varphi))}{(\delta-ik_0h+\delta_1\cos(2\varphi))^2}+ +\mathrm{H}_0^{(1)}(\lambda_p r)\left[\frac{2\delta_1\cos(2\varphi)}{(\delta-ik_0h+\delta_1\cos(2\varphi))}+\frac{\delta_1\sin(2\varphi)(\kappa+2\delta_1\sin 2\varphi)}{(\delta-ik_0h+\delta_1\cos(2\varphi))^2}\right]\Big\} \quad \text{(A1)}$$

$$B_r = \frac{i\cdot\mu_0(I\cdot s)}{2\pi\cdot r\cdot h}\left[\frac{\kappa+\delta_1\sin(2\varphi)}{\delta-ik_0h+\delta_1\cos(2\varphi)}\right] \quad \text{(A2)}$$

with (in Cartesian coordinates),

$$r=\sqrt{x^2+y^2} \quad \text{(A3)}$$

$$Z=\begin{pmatrix} Z_{xx} & Z_{xy}\\ Z_{yx} & Z_{yy}\end{pmatrix} \quad \text{(A4)}$$

$$\delta=\frac{Z_{yx}-Z_{xy}}{2\cdot Z_0} \quad \text{(A5)}$$

$$\delta_1=\frac{Z_{yx}+Z_{xy}}{2\cdot Z_0} \quad \text{(A6)}$$

$$\kappa=\frac{Z_{xx}}{Z_0}. \quad \text{(A7)}$$

Note that the field angle θ dependence enters in the expression of the upper boundary impedance Z. Here Z_0 stands for the impedance of free space, and Z is the matrix representing the impedance of the atmosphere-ionosphere interface in case of an inhomogeneous and anisotropic ionosphere, r is the distance between source and observation, h is the height of the wave guide, $I\cdot s$ is the source current moment, $\mathrm{H}_0^{(1)}$ is the zero order first Hankel function, θ is the Earth's magnetic field inclination angle's complement to 90°, φ is the angle between the k_0-wave vector and the normal to the magnetic meridian, the latter coinciding with the Y- and Z-axis of our coordinate system. The expressions are valid as long as $k_0 r \ll 1$, $r > h$, $k_0 n_{1,2} r \gg 1$, with $n_{1,2}$ the refractive indexes of normal waves in the ionosphere, respectively.

The formula for λ_p has the dimension of k_0 and is given by:

$$\lambda_p = \frac{k_0\sqrt{\delta-ik_0h}}{\sqrt{\delta-ik_0h+\delta_1\cos(2\varphi)}} \sqrt{1+\frac{i}{k_0h}\frac{\delta^2+\kappa^2-\delta_1^2-ik_0h\delta}{\delta-ik_0h}} \quad . \quad \text{(A8)}$$

In the numerical simulation, the iteration for estimating Z starts at a height of 1000 km and computes the lower boundary impedance by inputting the impedance at the upper boundary in 5 km wide layer steps down to 80 km. The

impedance matrix elements involves expressions of polarization parameters $P_{1,2}$, defined by the electric field components, E_x and E_y, of the two normal modes in an anisotropic plasma.

$$\hat{Z}(0)=\left[\hat{P}_e-\hat{P}_e\hat{E}(\hat{P}_e+\hat{Z}(d)\hat{P}_m\hat{Y})^{-1}(\hat{P}_e-\hat{Z}(d)\hat{P}_m\hat{Y})\hat{E}\right]\times$$
$$\times\left[\hat{P}_m\hat{Y}\hat{E}(\hat{P}_e+\hat{Z}(d)\hat{P}_m\hat{Y})^{-1}(\hat{P}_e-\hat{Z}(d)\hat{P}_m\hat{Y})\hat{E}+\hat{P}_m\hat{Y}\right]^{-1} \quad \text{(A9)}$$

$$\hat{P}_e=\begin{pmatrix}1 & 1\\ P_1 & P_2\end{pmatrix};\quad \frac{E_y}{E_x}=P_{1,2};\quad \hat{P}_m=\begin{pmatrix}-P_1 & -P_2\\ 1 & 1\end{pmatrix};$$
$$\hat{Y}=\begin{pmatrix}n_1 & 0\\ 0 & n_2\end{pmatrix};\quad \hat{E}=\begin{pmatrix}e^{-ik_1d} & 0\\ 0 & e^{-ik_2d}\end{pmatrix} \quad \text{(A10)}$$

The expressions for the refractive indices of the two normal modes in a inhomogeneous, anisotropic plasma are taken from V. L. Ginzburg: The Propagation of Electromagnetic Waves in Plasmas, Pergamon Press, Oxford (1970).

Acknowledgements. The author T. B. thanks the organizers for financial support allowing him to participate in the International Symposium of Aeronomy, ISEA-12, hold on the Island of Crete, Greece, 18–24 May 2008. The work of E. N. E. was done with support of RFBR (project 07-02-01189). A brief inspection of World Wide Lightning Location (WWLL) network data was kindly allowed by the Sodankylä Geophysical Observatory which presently operates a WWLL station.

Topical Editor K. Kauristie thanks A. Yahnin and T. Yeoman for their help in evaluating this paper.

References

Belyaev, P. P., Polyakov, S. V., Rapoport, V. O., and Trakhtengerts, V. Y.: Discovery of resonance structure in the spectrum of atmospheric electromagnetic background noise in the range of short-period geomagnetic pulsations, Doklady Akademii Nauk SSSR, 297, 840–846, 1987.

Belyaev, P. P., Polyakov, S. V., Rapoport, V. O., and Trakhtengerts, V. Y.: Theory of the formation of resonance structure in the spectrum of atmospheric electromagnetic background noise in the range of short-period geomagnetic pulsations, Radiophizik, 32, 802–810, 1989.

Belyaev, P. P., Polyakov, S. V., Rappoport, V. O., and Trakhtengerts, V. Y.: The ionospheric Alfvén resonator, J. Atmos. Terr. Phys., 52, 781–789, 1990.

Bösinger, T., Pashin, A. B., Kero, A., Pollari, P., Belyaev, P. P., Rietveld, M., Turunen T., and Kangas, J.: Generation of artificial magnetic pulsations in the Pc1 frequency range by periodic heating of the Earth's ionosphere: indications of Ionospheric Alfvén Resonator effects, J. Atmos. Solar-Terr. Phys., 62, 277–297, 2000.

Bösinger, T., Haldoupis, C., Belyaev, P. P., Yakunin, M. N., Semenova, N. N., Demekhov, A. G., and Angelopoulos, V.: Spectral properties of the ionospheric Alfvén resonator observed at a low latitude station (L=1.3), J. Geophys. Res. A, 107(A10), 1281, doi:10.1029/2001JA005076, 2002.

Bösinger, T., Demekhov, A. G., and Trakhtengerts, V. Y.: Fine structure in ionospheric Alfvén resonator spectra observed at low latitude (L=1.3), Geophys. Res. Lett., 31, L18802, doi:10.1029/2004GL020777, 2004.

Bösinger, T. and Shalimov, S. L.: On ULF signatures of lightning discharges, Space Sci. Rev., 137, 521–532, doi:10.1007/s11214-008-9333-4. 2008.

Demekhov, A. G., Belyaev, P. P., Isaev, S. V., Manninen, J., and Kangas, K.: Modeling the diurnal evolution of the resonance spectral structure of the atmospheric noise background in the Pc 1 frequency range, J. Atmos. Sol.-Terr. Phys., 62, 257–265, 2000.

Ermakova, E. N., Kotik, D. S., Polyakov, S. V., and Shchennikov, A. V.: On a mechanism forming a broadband maximum in the spectrum of background noise at frequencies 2–6 Hz, Radiophysics and Quantum Electronics, 50(7), 555–569, 2007.

Ermakova, E. N., Kotik, D. S., and Polyakov, S. V.: Studying specific features of the resonance structure of the background noise spectrum in the frequency range 1–10 Hz with allowance for the slope of the Earth's magnetic field, Radiophysics and Quantum Electronics, 51(7), 519–527, 2008.

Hebden, S. R., Robinson, T. R., Wright, D. M., Yeoman, T., Raita, T., and Bösinger, T.: A quantitative analysis of the diurnal evolution of Ionospheric Alfvn resonator magnetic resonance features and calculation of changing IAR parameters, Ann. Geophys., 23, 1711–1721, 2005, http://www.ann-geophys.net/23/1711/2005/.

Lyons, W. A., Uliasz, M., and Nelson, T.: Climatology of large peak current cloud-to-ground lightning flashes in the contiguous United States, Mon Weather Rev., 126, 2217–2233, 1998.

Lysak, R. L.: Generalized model of the Ionospheric Alfvén Resonator, in: Auroral Plasma Dynamics, Geophys. Monogr. Ser., vol. 80, 1993. edited by: Lysak, R. L., pp. 121–128, AGU, Washington, D.C., 1993.

Odzimek, A., Kułak, A., Michalec, A., and Kubisz, J.: An automatic method to determine the frequency scale of the ionospheric Alfvén resonator using data from Hylaty station, Poland, Ann. Geophys., 24, 2151–2158, 2006, http://www.ann-geophys.net/24/2151/2006/.

Pokhotelov, O. A., Feygin, F. Z., Khabazin, Y. G., Khruschev, V. V., Bösinger, T., Kangas, J., and Prikner, K.: Observations of IAR spectral resonance structures at a large triangle of geophysical observatories, Proc. of the XXVI Seminar "Physics of Auroral Phenomena", Apatity, pp. 123–126, 2003.

Pokhotelov, O. A., Onishchenko, O. G., Sagdeev, R. Z., and Treumann, R. A.: Nonlinear dynamics of inertial Alfvén waves in the upper ionosphere: Parametric generation of electrostatic convective cells, J. Geophys. Res., 108(A7), 1291, doi:10.1029/2003JA009888, 2003.

Polyakov, S. V.: On properties of an ionospheric Alfvén resonator, Symposium KAPG on Solar-Terrestrial Physics, 3, 72–73, Nauka, Moscow, 1976.

Polyakov, S. V. and Rapoport, V. O.: Ionospheric Alfvén resonator, Geomagn. Aeron., 21, 816–822, 1981.

Polyakov, S. V., Ermakova, E. N., Polyakov, A. S., and Yakunin, M. N.: The spectrum and polarization forming the background ultra low electromagnetic noise on earth surface, Geomagnetizm i aeronomija, 43(N2), 240–247, 2003.

Reinisch, B. W., Nsumei, P., Huang, X., and Bilitza, D. K.: Modeling the F2 topside and plasmasphere for IRI using IMAGE/RPI

and ISIS data, Adv. Space Res., 39, 731–738, 2007.

Semenova, N. V. and Yahnin, A. G.: Diurnal behaviour of the ionospheric Alfvén resonator signatures as observed at high latitude observatory Barentsburg (L=15), Ann. Geophys., 26, 2245–2251, 2008, http://www.ann-geophys.net/26/2245/2008/.

Scoffield, H. C., Yeoman, T. K., Robinson, T. R., Baddeley, L. J., Dhillon, R. S., Wright, D. M., Raita, T., and Turunen, T.: First results of artificial stimulation of the ionospheric Alfvén resonator at 78° N, Geophys. Res Lett., 33, L19103, doi:10.1029/2006GL027384, 2006.

Shalimov, S. and Bösinger, T.: On distant excitation of the ionospheric Alfvén resonator by positive cloud-to-ground lightning discharges, J. Geophys. Res., 113, A02303, doi:10.1029/2007JA012614, 2008.

Sobchakov, L. A., Polyakov, S. V., and Astakhova, N. L.: Excitation of electromagnetic waves in a plane waveguide with anisotropic upper wall, Radiophysics and Quantum Electronics, 46(12), 918–927, 2003.

Sukhorukov, A. I. and Stubbe, P.: Excitation of the ionospheric Alfven resonator by strong lightning discharges, Geophys. Res. Lett., 24, 829–832, doi:10.1029/97GL00807, 1997.

Surkov, V. V., Pokhotelov, O. A., Parrot, M., Fedorov, E. N., and Hayakawa, M.: Excitation of the ionospheric resonance cavity by neutral winds at middle latitudes, Ann. Geophys., 22, 2877–2889, 2004, http://www.ann-geophys.net/22/2877/2004/.

Surkov, V. V., Hayakawa, M., Schekotov, A. J., Fedorov, E. N., and Molchanov, O. A.: Ionospheric Alfvén resonator excitation due to nearby thunderstorms, J. Geophys. Res., 111, A01303, doi:10.1029/2005JA011320, 2006.

Trakhtengerts, V. Y. and Feldstein, A. Y.: Turbulent Alfvén boundary layer in the polar ionosphere: J. Geophys. Res., 96(A11), 19363–19374, 1991.

Wait, J. R.: Cavity resonances for a spherical Earth with a concentric anisotropic shell, J. Atmos. Terr. Phys., 27, 81–89, 1965.